



Efficient growth of ordered thin oxide films on Ni(1 1 1) by NO₂ oxidation

B.S. Yeo, Z.H. Chen, W.S. Sim *

Department of Chemistry, National University of Singapore, Kent Ridge, Singapore 119260, Singapore

Received 17 January 2004; accepted for publication 24 March 2004

Abstract

The efficient growth of ordered thin oxide films on Ni(1 1 1) using low NO₂ gas exposures under ultrahigh vacuum conditions has been achieved. The reaction mechanism of NO₂ on Ni(111) at 500–600 K changes from total decomposition to partial dissociation into NO and O after a critical surface adatom coverage has been attained. Auger electron spectroscopy (AES) and low energy electron diffraction (LEED) reveal the creation of an intermediate NiO(100) phase, followed by the eventual formation of clean NiO(111) overlayers. Reflection absorption infrared spectroscopy (RAIRS) using CO molecules as probes of the surface adsorption sites present confirms the conversion of Ni⁰ to Ni²⁺ during the oxidation process.

© 2004 Elsevier B.V. All rights reserved.

Keywords: Nickel oxides; Nitrogen oxides; Auger electron spectroscopy; Low energy electron diffraction (LEED); Infrared absorption spectroscopy; Low index single crystal surfaces; Growth

1. Introduction

Understanding the properties and reactivity of NiO surfaces is essential from a technological and commercial standpoint because of its utility as a key material in many catalytic processes [1]. Due to the insulating nature of oxide materials that results in sample charging problems when probed with electron-based spectroscopies, surface science studies are normally conducted on NiO thin films prepared by the direct oxidation of Ni single crystal surfaces with molecular O₂. The general

mechanism for this process involves dissociative adsorption, oxide island formation and thick oxide growth. On Ni(111), the formation of ordered $p(2 \times 2)$ and $p(\sqrt{3} \times \sqrt{3})R30^\circ$ O overlayers has been observed during the initial chemisorption stages. NiO islands then grow and amalgamate until the entire surface is oxidized [2].

This method of synthesizing metal oxide thin films requires relatively large gas exposures as the probability of dissociative O₂ chemisorption tends to decrease rapidly with increasing surface O coverages, especially for Ni surfaces [3]. NO₂ is a much more efficient oxidant as it is able to maintain a high dissociative sticking probability to yield NO and atomic O even in the presence of large concentrations of surface O [4,5]. This property makes

* Corresponding author. Tel.: +65-6874-2680; fax: +65-6779-1691.

E-mail address: chmsimws@nus.edu.sg (W.S. Sim).

it particularly useful for oxidation reactions under ultrahigh vacuum (UHV) conditions, where practical considerations require the minimization of gas loading in the system. NO_2 oxidation has been used to successfully fabricate metal oxide thin films on $\text{Mo}(110)$ [6], $\text{Ru}(001)$ [7], $\text{Pd}(111)$ [5], $\text{Cu}(100)$ [8] and $\text{Ag}(111)$ [9,10] under much milder conditions than that needed for O_2 oxidation.

In this work, Auger electron spectroscopy (AES), low energy electron diffraction (LEED) and reflection absorption infrared spectroscopy (RAIRS) have been utilized in tandem to investigate the oxidation of $\text{Ni}(111)$ by NO_2 . It will be shown here that NO_2 decomposes readily on $\text{Ni}(111)$ to give atomic O that undergoes facile reaction with the metal substrate to produce clean and ordered $\text{NiO}(111)$ thin films.

2. Experimental

All experiments were performed in a stainless steel UHV chamber with a base pressure $<2 \times 10^{-10}$ Torr that has been described in detail elsewhere [11]. The $\text{Ni}(111)$ sample was cleaned by repeated cycles of Ar ion sputtering and annealing, with its cleanliness and surface structure verified by the absence of any detectable contaminant AES signals and the observation of a sharp hexagonal LEED pattern with little background intensity. The oxidation process was carried out by exposing the clean $\text{Ni}(111)$ crystal held at a temperature of 500 K to NO_2 (Soxal, 99.5%) dosed through a variable leak valve, followed by annealing to 600 K to desorb any molecular species present on the surface. All LEED images and AES spectra were collected at 300 K while RAIRS was performed at 120 K under an ambient CO background pressure of 5×10^{-8} Torr in order to maintain a saturation population of CO on Ni adsorption sites that may be energetically unfavourable towards Ni–CO bonding.

3. Results and discussion

AES was employed to quantify the elemental composition of the oxide film grown on the

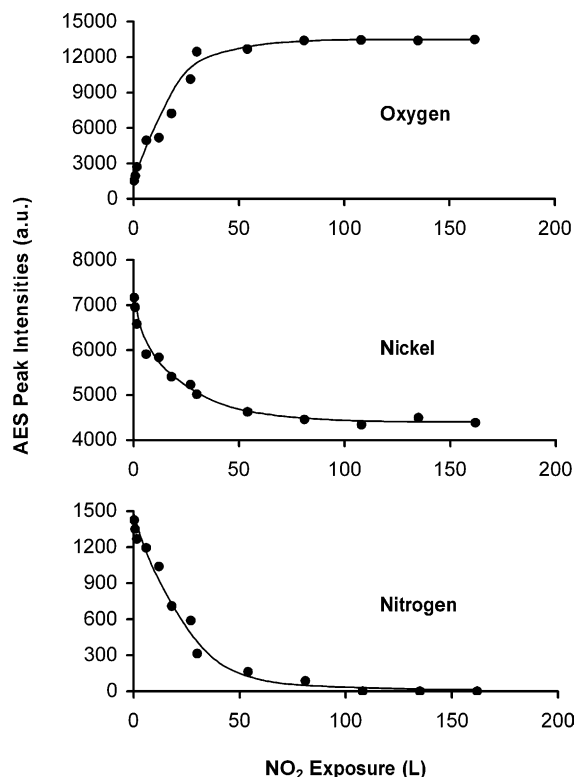


Fig. 1. Plots of AES peak intensities of the O_{510} (KLL), Ni_{848} (LMM) and N_{352} (KLL) signals as a function NO_2 exposure.

$\text{Ni}(111)$ sample using the peak-to-peak heights of the O_{510} (KLL), Ni_{848} (LMM) and N_{352} (KLL) signals (dN/dE). In Fig. 1, the intensities of the O, Ni and N signals measured during the oxidation process are plotted as a function of NO_2 exposure, with the common feature of all three plots being the concerted increase (O) or decrease (Ni and N) followed by plateauing of the AES signals at >80 L NO_2 exposure. Previous reports have indicated that the growth of NiO thin films on $\text{Ni}(111)$ can be self-limiting [3], and similar mechanisms may be operating in the present case.

Assuming that n layers of NiO grow uniformly in a (111)-orientation on the $\text{Ni}(111)$ substrate such that there is an exponential attenuation of the AES intensities with film thickness, the ratio of the O to Ni AES signals may be expressed as:

$$\frac{I_{\text{O}}}{I_{\text{Ni}}} = \frac{S_{\text{O}}}{S_{\text{Ni}}} \times \frac{\sum_{i=1}^n C_{\text{O,oxide}} \exp(- (i-1)x_{\text{oxide}} \cos \theta / \lambda_{\text{O,oxide}})}{\sum_{i=1}^n \left(C_{\text{Ni,oxide}} \exp(- (i-1)x_{\text{oxide}} \cos \theta / \lambda_{\text{Ni,oxide}}) + \exp(- nx_{\text{oxide}} \cos \theta / \lambda_{\text{Ni,oxide}}) \sum_{j=1}^{\infty} C_{\text{Ni,metal}} \exp(- (j-1)x_{\text{metal}} \cos \theta / \lambda_{\text{Ni,metal}}) \right)}$$

For the NiO(111) layers, the concentrations of O and Ni are $C_{\text{O,oxide}} = C_{\text{Ni,oxide}} = 0.133 \text{ ions } \text{\AA}^{-2}$, the interlayer distance $x_{\text{oxide}} = 2.41 \text{ \AA}$, and the electron mean free paths for the O and Ni electrons are $\lambda_{\text{O,oxide}} = 9.5 \text{ \AA}$ and $\lambda_{\text{Ni,oxide}} = 10.8 \text{ \AA}$ respectively [12]. The corresponding values for the Ni(111) substrate are $C_{\text{Ni,metal}} = 0.186 \text{ atoms } \text{\AA}^{-2}$, $x_{\text{metal}} = 2.03 \text{ \AA}$, and $\lambda_{\text{Ni,metal}} = 10.2 \text{ \AA}$ [12]. Using a collection angle $\theta = 90^\circ$ and a relative sensitivity factor $S_{\text{O}}/S_{\text{Ni}} = 4$ calibrated for our retarding field analyzer, the O to Ni AES intensity ratio $I_{\text{O}}/I_{\text{Ni}} = 3.05$ at saturation ($>80 \text{ L}$) NO_2 exposure yields a NiO film thickness of 9–10 layers. This result agrees well with the reported thicknesses of NiO films grown using O_2 gas as the oxidant, which range from 3–4 layers to 8–21 layers when oxidation was carried out at 300 K [3,12] and 570 K [13] respectively.

The N AES signal is observed to have the highest intensity at the lowest NO_2 exposure, and this can be attributed to the presence of atomic N formed by the complete decomposition of NO_2 on Ni(111) at the earliest stages of the oxidation process. This probably occurs via an NO intermediate species, which is itself known to dissociate on clean Ni(111) but remains intact in the presence of preadsorbed O [14]. As the oxidation proceeds, the buildup of O and N adatoms in the overlayer eventually inhibits the NO dissociation [15] and results in a mechanism switch from complete to partial NO_2 decomposition, with the NO formed desorbing under the experimental conditions ($>500 \text{ K}$) [16]. The rapid decay of the N AES signal indicates that the atomic N formed is only embedded in the initial chemisorbed overlayer and absent in the growing NiO film.

LEED images at 84 eV of the various ordered surface structures present during the NO_2 oxidation process are shown in Fig. 2. The clean Ni(111) surface is characterized by a regular hexagonal array of six sharp spots (Fig. 2(a)).

Upon 0.3 L NO_2 exposure, a complex LEED pattern reminiscent of that obtained when NO dissociates on Ni(111) into an overlayer of coadsorbed O and N is observed (Fig. 2(b)) [14]. At 18 L NO_2 exposure, the LEED image consists of the six Ni(111) substrate spots, a smaller hexagonal ring of six spots oriented parallel to the original hexagonal substrate array, and two dodecagonal rings of 24 spots (Figs. 2(c) and 3). The attenuation of the complex LEED pattern suggests disordering of the O and N overlayer. Above 80 L NO_2 exposure, the substrate spots have disappeared, the two rings of 24 spots have also faded, while the new hexagonal ring of six spots has become noticeably brighter (Fig. 2(d)).

The $\sim 15\%$ reduction in the reciprocal surface lattice parameter of the structure giving rise to these six spots with respect to that of the Ni(111) substrate is in excellent agreement with the difference in lattice constants of NiO (4.17 \AA) and Ni (3.52 \AA). In addition, the hexagonal LEED pattern coupled with the absence of any half-order spots implies that ordered layers with a NiO(111)- $p(1 \times 1)$ structure have been formed. The positions of the observed LEED spots are also consistent with the preferred growth behaviour of NiO(111) on Ni(111), where the LEED patterns of both the oxide overlayers and the substrate are known to be aligned [17].

The intensity attenuation observed for the two rings of 24 spots as the oxidation proceeds indicates that they originate from an intermediate type structure, possibly formed at the interfacial region between the NiO(111) overlayers and Ni(111) substrate. The positions of these spots are consistent with the presence of three 120° rotational domains of NiO(100), which give rise to a reciprocal surface lattice parameter contraction of $\sim 28\%$ with respect to the Ni(111) substrate, as shown schematically in Fig. 3. These domain structures have also been observed by scanning tunneling microscopy (STM)

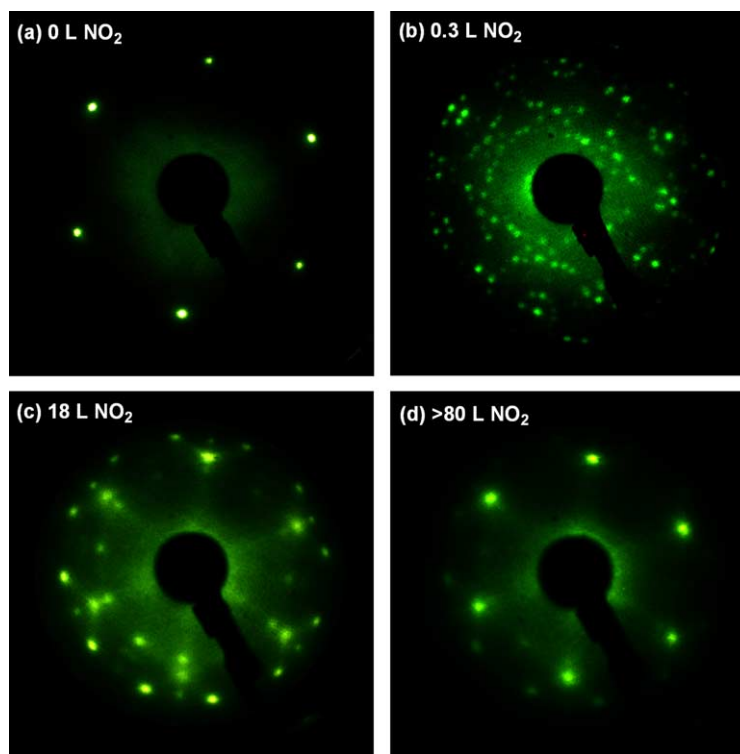


Fig. 2. LEED images of Ni(111) at 84 eV after oxidation by (a) 0 L, (b) 0.3 L, (c) 18 L and (d) >80 L NO_2 .

during the initial stages of NiO(111) growth on Ni(111) via O_2 oxidation [18].

The $\nu(\text{CO})$ frequency of CO adsorbed on the Ni(111) surface at different stages of the oxidation process gives valuable information about the oxidation state of the Ni atoms present as it is a sensitive function of the degree of electron transfer between the CO molecular orbitals and the metallic adsorption sites. In general, the $\nu(\text{CO})$ frequency increases as the metal atom becomes more positively charged [19]. This generalization is applicable to the current work where the relative invariance of the $\nu(\text{CO})$ frequencies with band size on the oxidized surface phases indicates that the CO exists as islands of constant local coverage with the same degree of dipole coupling that is independent of total surface coverage within each phase. Fig. 4 shows a series of RAIR spectra for saturation coverages of CO adsorbed on Ni(111) under 5×10^{-8} Torr ambient gas pressure at 120 K after oxidation with various NO_2 exposures. The

clean surface has two $\nu(\text{CO})$ bands at 2054 and 1917 cm^{-1} , consistent with CO adsorbed at on-top and two-fold bridging Ni^0 sites respectively in the $p(\sqrt{7} \times \sqrt{7})R19.1^\circ$ structure [20,21].

After 0.3 L NO_2 exposure, two new $\nu(\text{CO})$ bands are observed at 2126 and 2090 cm^{-1} , together with broad and weak absorption features centered around 2066 and 1920 cm^{-1} that arise from CO adsorbed on residual patches of clean Ni(111) [22]. The AES and LEED data at this stage indicate that O and N adatoms are both present on the surface, probably as separate phases given that the N–N and N–O repulsive pairwise lateral interaction energies are twice that for O–O [15]. The complex LEED pattern then presumably arises from six domain orientations of a $c(5\sqrt{3} \times 9)\text{rect-N}$ structure, in which the N atoms occupy four-fold hollow sites in a reconstructed Ni(100)- $c(2 \times 2)$ -2N-like top layer [23]. The Ni(100)- $c(2 \times 2)$ -2O surface has been reported to be inert towards CO adsorption [24], and we propose that a similar

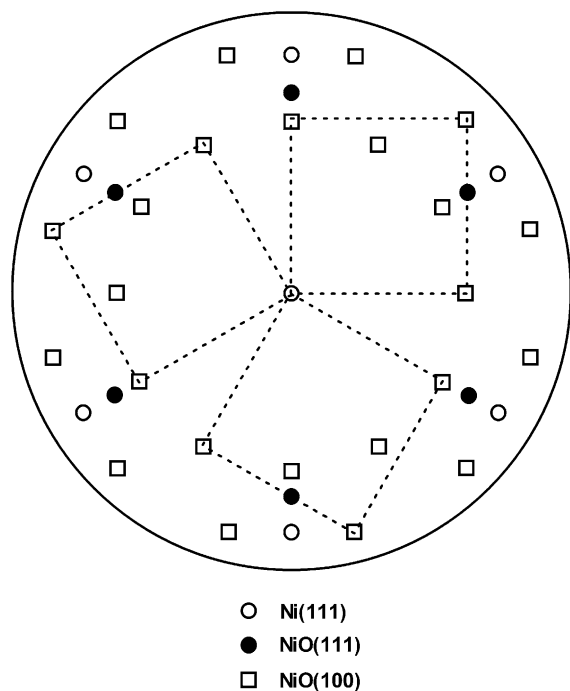


Fig. 3. Schematic diagram of the LEED spots observed in Fig. 2(c) for Ni(111) at 84 eV after oxidation by 18 L NO₂, showing the three 120° rotational domains of NiO(100).

situation occurs here. The $\nu(\text{CO})$ band at 2090 cm^{-1} is characteristic of CO adsorbed on-top of O-perturbed Ni⁰ atoms [22]. However, the absence of any other known LEED patterns associated with adsorbed O on Ni(111) suggests that the O adlayer is in a disordered state. The $\nu(\text{CO})$ band at 2126 cm^{-1} lies approximately midway between that of CO adsorbed on O-perturbed Ni⁰ and fully oxidized Ni²⁺ sites. On the basis of electronic considerations, it can be reasonably ascribed to CO linearly bonded on-top of partially oxidized Ni ^{$\delta+$} sites. This assignment is in agreement with infrared spectroscopic studies of CO adsorption on NiO supported on Ni(111) [25] and Al₂O₃ [19,26], where $\nu(\text{CO})$ bands at 2120–2124 cm^{-1} were also postulated to originate from CO adsorbed on such Ni ^{$\delta+$} sites.

At 18 L NO₂ exposure, the bands observed earlier are attenuated and a new $\nu(\text{CO})$ band appears at 2142 cm^{-1} , which grows to become the main feature in the RAIR spectrum at NO₂ exposures >80 L. This sharp and well-defined band may

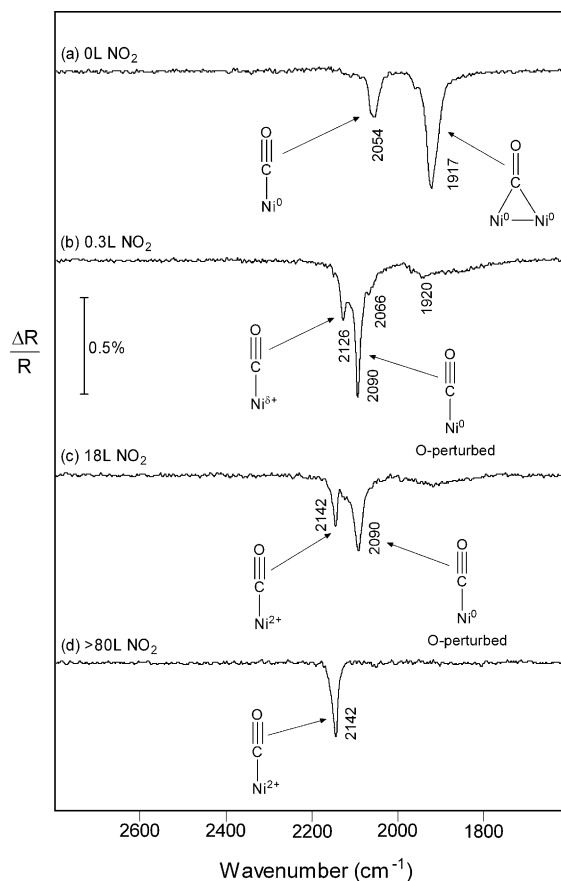


Fig. 4. RAIR spectra of Ni(111) under an ambient CO gas pressure of 5×10^{-8} Torr at 120 K after oxidation by (a) 0 L, (b) 0.3 L, (c) 18 L and (d) >80 L NO₂.

be assigned to CO adsorbed on-top of Ni²⁺ sites in the NiO(111) thin film. Its absorption frequency is consistent with the higher oxidation state of the Ni²⁺ substrate atoms, and in excellent agreement with previous infrared and high resolution electron energy loss spectroscopy (HREELS) studies of CO adsorption on NiO(111) thin films, which have also yielded $\nu(\text{CO})$ frequencies at ~ 2150 cm^{-1} for the Ni²⁺-bound species [27,28]. The efficacy of NO₂ in effecting the complete and homogeneous oxidation of the Ni(111) surface is demonstrated by the absence of any other $\nu(\text{CO})$ absorption bands between 1800 and 2130 cm^{-1} in the RAIR spectra at >80 L NO₂ exposure. While the possibility of the oxidized surface being terminated with OH groups

from dissociative background adsorption of residual H_2O or H_2 cannot be completely ruled out, the presence of these coadsorbates does not appear to affect the chemisorption behaviour of CO on the oxidized surface [27].

The current results show that the reaction pathway of NO_2 on Ni(111) rapidly switches from complete decomposition on the clean surface to partial dissociation in the presence of adsorbed O and N. The net result is the inclusion of a small quantity of N atoms into a bridging interfacial layer, and the subsequent growth of N-free ordered NiO thin films of predominantly (111) orientation. The crucial factor in this behaviour is the change from dissociative to molecular chemisorption of the NO intermediate on Ni when the dissociation products reach a critical surface coverage due to strong repulsive interactions between the O and N adatoms [15]. Except for Mo(110) [6], previous studies of NO_2 oxidation of transition metal surfaces have generally not made any mention of the presence of N in the oxide films grown [5,7–10]. Assuming that similar mechanisms exist in some of these cases involving the more reactive transition metals whose clean surfaces are known to dissociate NO, then any N contamination would be expected to be localized within the interfacial region between the substrate and the growing oxide film and may not have been detected. The amount of N incorporated depends on the propensity of the clean metal surface towards NO dissociation, and can probably be minimized by covering the surface with O adatoms from an O_2 gas source beforehand.

4. Conclusions

In summary, we have grown clean and ordered NiO(111) thin films on a Ni(111) substrate under UHV conditions using NO_2 as the oxidant at relatively low gas exposures. Detailed characterization of the growth process with AES, LEED and RAIRS has revealed an underlying oxidation mechanism whereby the switch from dissociative to molecular chemisorption of an NO intermediate species is the key towards the formation of pure N-free oxide films.

Acknowledgements

We acknowledge financial support for this work from the National University of Singapore (Grant No. R-143-000-074-112).

References

- [1] A. Bielanski, J. Haber, Oxygen in Catalysis, Marcel Dekker, New York, 1990.
- [2] C.R. Brundle, J.Q. Broughton, in: D.A. King, D.P. Woodruff (Eds.), The Chemical Physics of Solid Surfaces and Heterogeneous Catalysis, Elsevier, Amsterdam, vol. 3A, 1990, p. 131.
- [3] J.T. Stuckless, C.E. Wartnaby, N. Al Sarraf, S. Dixon-Warren, M. Kovar, D.A. King, J. Chem. Phys. 106 (1997) 2012.
- [4] B.A. Banse, B.E. Koel, Surf. Sci. 232 (1990) 275.
- [5] G. Zheng, E.I. Altman, Surf. Sci. 462 (2000) 151.
- [6] T. Jirsak, M. Kuhn, J.A. Rodriguez, Surf. Sci. 457 (2000) 254.
- [7] W.J. Mitchell, W.H. Weinberg, J. Chem. Phys. 104 (1996) 9127.
- [8] A.B. Gurevich, B.E. Bent, A.V. Teplyakov, J.G. Chen, Surf. Sci. 442 (1999) L971.
- [9] S.R. Bare, K. Griffiths, W.N. Lennard, H.T. Tang, Surf. Sci. 342 (1995) 185.
- [10] C.I. Carlisle, T. Fujimoto, W.S. Sim, D.A. King, Surf. Sci. 470 (2000) 15.
- [11] B.S. Yeo, Z.H. Chen, W.S. Sim, Langmuir 19 (2003) 2787.
- [12] M.A. Langell, M.H. Nassir, J. Phys. Chem. 99 (1995) 4162.
- [13] F. Rohr, K. Wirth, J. Libuda, D. Cappus, M. Baeumer, H.J. Freund, Surf. Sci. 315 (1994) L977.
- [14] H. Conrad, G. Ertl, J. Kuppers, E.E. Latta, Surf. Sci. 50 (1975) 296.
- [15] L. Vattuone, Y.Y. Yeo, D.A. King, Catal. Lett. 41 (1996) 119.
- [16] D. Cappus, C. Xu, D. Ehrlich, B. Dillmann, C.A.J. Ventrice, K. Al Shamery, H. Kuhlbeck, H.J. Freund, Chem. Phys. 177 (1993) 533.
- [17] N. Kitakatsu, V. Maurice, P. Marcus, Surf. Sci. 411 (1998) 215.
- [18] S. Hildebrandt, C. Hagendorf, T. Doege, C. Jecksties, R. Kulla, H. Neddermeyer, T. Uttich, J. Vac. Sci. Technol. A 18 (2000) 1010.
- [19] J.B. Peri, J. Catal. 86 (1984) 84.
- [20] G. Held, J. Schuler, W. Sklarek, H.P. Steinruck, Surf. Sci. 398 (1998) 154.
- [21] L. Surnev, Z. Xu, J.T. Yates, Surf. Sci. 201 (1988) 1.
- [22] Z. Xu, L. Surnev, K.J. Uram, J.T. Yates, Surf. Sci. 292 (1993) 235.
- [23] D.E. Gardin, J.D. Batteas, M.A. Van Hove, G.A. Somorjai, Surf. Sci. 296 (1993) 25.

- [24] S. Andersson, *Solid State Commun.* 24 (1977) 183.
- [25] J. Yoshinobu, T.H. Ballinger, Z. Xu, H.J. Jansch, M.I. Zaki, J. Xu, J.T. Yates, *Surf. Sci.* 255 (1991) 295.
- [26] C. Xu, Q. Guo, D.W. Goodman, *Catal. Lett.* 41 (1996) 21.
- [27] M. Schonnenbeck, D. Cappus, J. Klinkmann, H.J. Freund, L.G.M. Petterson, P.S. Bagus, *Surf. Sci.* 347 (1996) 337.
- [28] T. Matsumoto, A. Bandara, J. Kubota, C. Hirose, K. Domen, *J. Phys. Chem. B* 102 (1998) 2979.